International Journal of Heat and Technology
Vol. 40, No. 3, June, 2022, pp. 665-670
Journal homepage: http://iieta.org/journals/ijht

CHECK TEMPERATURE: A Small-Scale Elastocaloric Device for the Cooling of the Electronic Circuits

Luca Cirillo, Adriana Greco, Claudia Masselli*

Department of Industrial Engineering, University of Naples Federico II, P.le Tecchio 80, 80125 Naples, Italy

Corresponding Author Email: claudia.masselli@unina.it

7th AIGE/IIETA International conference and 16th AIGE Conference-SPECIAL ISSUE

https://doi.org/10.18280/ijht.400302

Received: 5 May 2022
Accepted: 12 June 2022

Keywords:
elastocaloric effect, not-in-kind technology, prototype, caloric cooling, shape-memory alloys

ABSTRACT

Elastocaloric is a technology to the class of solid-state cooling based on caloric-effects have attracted great interest in recent years, representing a new and viable alternative to vapour-compression. The physical phenomenon on which elastocaloric systems are based is elastocaloric effect: a physical-thermal phenomenon manifesting in some materials called shape memory alloys where, consequently to an adiabatic variation of the intensity of an external field, a temperature variation (ΔT_{ad}), occurs. If the intensity of the field is increasing, a temperature rise is observed in the elastocaloric material; conversely, to a decreasing intensity a temperature fall corresponds. Controlling the temperature of electronic equipment is also essential and, currently, there are not elastocaloric devices specifically addressed to this application. In this context CHECK TEMPERATURE (acronym of "Controlling the Heating of Electronic Circuits: a Key-approach Through Elastocaloric Materials in a Prototype Employing them as Refrigerants of an AcTive Ultrasmall Refrigerator") project was born: the main purpose of this project is to develop an elastocaloric device targeted on miniature scale for environmentally friendly cooling of electronic components. In this paper all the aspect concerning the development are described.

1. INTRODUCTION

ElastoCaloric (EC) Cooling is part of the wider class of Solid-state cooling, air conditioning and heat pumping based on caloric effect, defined as Not-In-Kind Heat Pumping alternative to Vapor Compression (VC) [1]. The Montreal [2] and Kyoto Protocols [3] in 1987 and 1997, established rules for progressively phasing out these substances: Chloro-FluoroCarbons (CFCs) HydroChloroFluoroCarbons (HCFCs) were phased out in developed countries starting from 1996 [4-6], followed by HydroFluoroCarbons (HFCs) [7, 8], whose phasing out started in 2015 and is planned to get a 85% reduction in 2036. The needing to find novel technologies able to replace VC derives from the gradually phasing-out the Hydro-Fluoro-Carbons (HFCs) refrigerants because of their elevate GWP (Global Warming Potential) and widely utilized in VC coolers that nowadays are responsible of more than 20% of the world energy consumption. The most suitable replacement for HFCs lies in the class of HFOs (HydroFluoroOlefins), drop-in fluids also for already existing VC plants [9]. Otherwise, the technology can be completely restyled founding on renewable energy systems, through the employment of solar collectors for domestic hot water or for solar cooling air conditioning systems [10, 11]. Moreover, also the usage of geothermal energy [12] for earth to air heat exchangers can be a suitable solution for renewable heat pumps [13].

Apart systems based on renewable energy sources, there are caloric heat pumps that, utilizing refrigerants showing caloric effects and classified as zero-GWP because of their solid-state nature, do not provide direct contribution to Total Equivalent Warming Impact (TEWI); moreover, the energy efficiency 50-60% higher than VC [14] theoretically shown by caloric systems translates also into a much lower indirect contribution in terms of TEWI, compared to the VC ones [15-17]. Caloric systems can be based on magnetocaloric [18-20], electrocaloric [21, 22], elastocaloric [23] or barocaloric [24, 25], depending on the properties of the solid-state material and the forcing field.

The interest toward EC is very recent but the number of studies published, and the researchers involved is rapidly increasing. As detailed reported in the state of the art of this technology, widely illustrated in section 3, the international scientific community has presented about a dozen of EC prototypes for residential and commercial applications, but they are far from the final stage of commercialization.

Next to the above-cited application, another crucial field is the one related to the control of the temperature of electronic equipment. Currently, the CPU heatsinks have thermal powers to be disposed of 80 W and depending on the environmental conditions (e.g. hot summers) the probability of electrical and electronic failures increase considerably. Therefore, the need arises in developing new devices for temperature control capable in dissipating a huger heat amount. The specific electronic applications for which, rather than the traditional finned systems, a more sophisticated cooling system is required are data centres and converters located in power electronics. There are no EC cooling systems explicitly oriented on this application at the best of our knowledge.

The CHECK TEMPERATURE (acronym of "Controlling the Heating of Electronic Circuits: a Key-approach Through Elastocaloric Materials in a Prototype Employing them as Refrigerants of an AcTive Ultrasmall Refrigerator") project intends to develop the first EC device for the cooling of electronic applications. Additionally, it represents another step towards sustainable, light cooling of electronic circuits with cooling powers greater than the solid-to-solid EC types but relatively small dimensions. In this paper all the steps taken toward this goal are detailly illustrated.

2. ELASTOCALORIC EFFECT AND REFERENCE THERMODYNAMICAL CYCLE FOR COOLING

Elastocaloric effect is the phenomenon that allows the existence of EC technology. Elastocaloric effect is a phenomenon detected into Shape Memory Alloys (SMAs) and Shape Memory Polymers (SMPs): two class of polymers characterized by the properties of shape memory and superelasticity. The former is the capability from the material to memorize its shape under no solicitations and being able to come back after the remotion of a structural forcing field. The latter is related to elastocaloric effect though the latent heat that released/absorbed during the forward/reverse austenite-martensite phase transformations.

According to the graph plotted in Figure 1, under relaxing state (stress-free), the Shape Memory Alloy is initially fully austenite at the temperature on which the application starts.

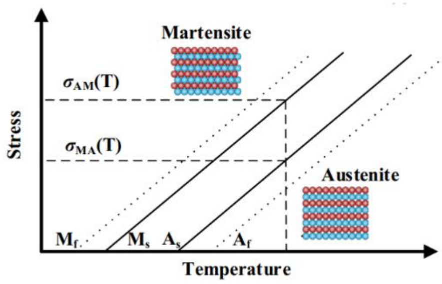

Figure 1. The Austenite-Martensite transformations in shape memory alloys

Then, through an operation of mechanical loading, a stress level begins to grow on the SMA; when the stress goes over a crucial level called Austenite-to-Martensite saturation stress of phase change ($\sigma_{AM}(T)$), the austenite starts to transform into the martensite phase. During the phase transformation, entropy reduces, and latent heat is released to the ambient. The dual phase change from martensite to austenite occurs when the stress coupled to the mechanical loading forced on the SMA, begins to decrease, thus falling down the Martensite-to-Austenite saturation stress of phase change ($\sigma_{MA}(T)$). Consequently, the SMA absorbs heat from the environment so realizing a cooling effect. σ_{AM} and σ_{MA} do not have the same value because of the hysteresis that characterizes the AM and MA transformation. Since these two phase changes are affected by hysteresis, consequently four are the temperatures characterizing them: A_f, A_s, M_f, M_s that represent the final and the starting temperatures into which the SMA has an austenite or martensite nature [26].

The adiabatic temperature change coupled with elastocaloric effect can be defined as follows:

$$\Delta T_{ad} = -\int_{\sigma_0}^{\sigma_1} \frac{T}{C}\left(\frac{\partial \varepsilon}{\partial T}\right)_{\sigma} d\sigma \quad (1)$$

where it is visible the intrinsic correlation by the forcing field σ (stress) and the variation of the intensity of the conjugate field ε (strain). Indeed, if the intensity of the field is increasing, a temperature rise is observed in the elastocaloric material; conversely, to a decreasing intensity a temperature fall corresponds [27].

The elastocaloric effect can be exploited into a thermodynamic cycle for cooling or heat pumping: the reference one is the inverse Brayton cycle to which the concept of active regeneration is applied to increase the maximum temperature span achievable in the EC system. So the most used cycle is called Active elastocaloric Regenerative refrigeration cycle (AeR) characterized by 4 phases, as visible in Figure 2(a) [28, 29]: loading, heat transfer (heating); unloading; heat transfer (cooling). The singularity is the double mansion entrusted to the SMA: in two steps is refrigerant and in the other two it behaves as a regenerator that thermally interacts with a hot and a cold heat exchanger. The goal is to subtract heat from the thermal load (cooling mode), represented by the cold side. The heat fluxes are vehiculated by an auxiliary fluid (generally air or water) that crosses the active elastocaloric regenerator.

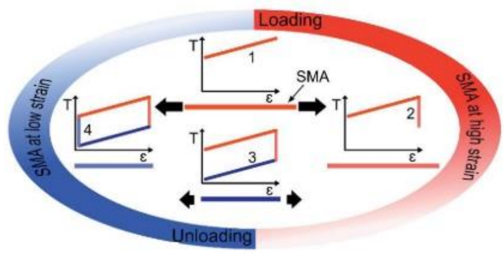

(a)

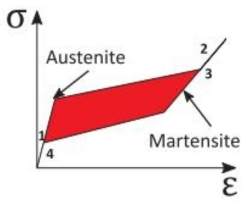

(b)

Figure 2. (a) Trend of the SMA temperature as a function of strain ε in the four-stage cycle; (b) corresponding stress-strain diagram

Loading: a mechanical is adiabatically employed to the SMA, whose intensity is sufficient to provoke the expected austenite/martensite phase change so to observe a growing in the SMA temperature (ΔT_{ad}).

Heat transfer (heating): the convective heat exchange generated by the flowing of the Heat Transfer Fluid (HTF) throughout the EC SMA has the consequence to heat resealing toward hot side since the fluid increase the temperature because of the exchange with the SMA.

Unloading: the mechanical load is removed by the SMA under adiabatic conditions and the temperature furtherly falls due to elastocaloric effect (ΔT_{ad}) (martensite to austenite phase change).

Heat transfer (cooling): the convective heat exchange generated by the flowing of the heat transfer fluid throughout the EC SMA has the consequence to warm the latter and cool the fluid that, once entering in the cold heat exchanger thus makes the heat remotion from the thermal load.

In Figure 2(b) in the stress-strain diagram are plotted the four steps of the AeR cycle. The area defined by the curves represents the unrecoverable work due to hysteresis.

Next to the AeR, the solid-to-sold thermal diode-based cycle is an alternative solution where, rather than through an HTF, the heat transfer is realized by means of solid-state materials able to change their thermal conductivity because of an external stimulus. With this solution the system can work under higher operation frequencies, but the maximum achievable temperature span coincides with ΔT_{ad}, the adiabatic temperature change of the employed refrigerant due to elastocaloric effect.

3. STATE OF THE ART OF THE ELASTOCLAORIC TECHNOLOGY

Elastocaloric is a class of solid-state technologies of recent interest. Magnetocaloric refrigeration is the most consolidated solid-state technology, as it was, about 25-30 years ago [30-32], the first to attract the interest of scientific community for the development of cooling applications because of the magnetocaloric effect of Gadolinium, the benchmark material, in room temperature range. To date, about 100 magnetocaloric prototypes have been developed but still few are close to being commercialized [33]. The major limitations are related to the energy performance characterized mostly by low values of the Coefficients of Performance (COPs), low cooling capacities and temperature jumps allowed. Anyhow, all the theoretical and numerical analysis carried out so far have given very encouraging results, demonstrating the possibility of large energy savings (from 30% to 60%) compared to traditional technologies. In the last decade, there was a progressive interest toward caloric refrigeration technologies, in particular toward the EC one, asserted to be the real breakthrough Non-Vapor-Compression technology [26], because of the colossal ΔT_{ad} induced by the deformation of a SMA by means of mechanical stress. Nowadays, research on EC cooling can be divided into three areas: a) the research of promising eCMs provided of giant temperature changes at room temperature and sufficiently long fatigue life; b) the development of smart and versatile models to operate in parallel with the experimental field to the purpose of optimizing the performances; c) the realization of novel and competitive experimental devices.

a) The EC benchmark material is the Nickel-Titanium (NiTi) binary alloy, the most investigated EC SMA because of its remarkable adiabatic temperature change (ΔT_{ad}) at room temperature: ΔT_{ad} of 25.5 K during loading and 17 K during unloading under 8.5% strain. Next to the binary Ni-Ti, ternary or quaternary Ni-Ti alloys are also very promising. With respect to the binary version, copper or vanadium addition to Ni-Ti alloys has the purpose to minimize the stress hysteresis and to enhance fatigue life [28]. Other popular SMA are the Cu-based as Cu-Zn and Cu-Sn, even if more interesting are the ternary alloys, e.g. Cu-Zn-Al because of the highest latent heat shown, i.e. ΔTad up to 15 K. The main con is the small fatigue life that strongly limits the possibility of being employed for commercial applications. Fe-based SMAs are not so promising like the former two classes because due of a much smaller latent heat rather than the other ones. [34]. The benchmark of the ECM is NiTi and the strain applied to the material cannot exceed 9% because the greater the induced stress is, the shorter the life-time of the material used before it cracks. The study of the life-time and the fatigue life is a fundamental aspect for the development of competitive devices and for this reason the development of new eCM s is a very important and it is a hot topic in the EC research.

b) One of the basic requirements is to find the most appropriate EC refrigerant due of a remarkable eCE and a fatigue life able to guarantee a huge number of cycles before the manifesting of cracks. Additionally, the shape and the dimensions of the eCMs mounted in a prototype, as well as the operating conditions (cycle frequency, speed of the HTF...) must be optimized. These aims could be achieved through the numerical modelling: the realization of a model able to predict the thermal and the energy performances of a device, could constitutes a guide tool to make a prototype working under the best conditions. Many are the models developed and published in open literature; most of them are one-dimensional [34]. Cirillo et al. [35, 36] realized a two-dimensional tool of a single bunch of EC wires based on finite-element method able to reproduce step by step the velocity and the pressure field of fluid, to predict more accurately the solid-to-fluid heat exchange. Through this tool the aspects related to the optimization of the frequency of the AeR cycle, the fluid velocity, the distance between two EC wires and their length were investigated.

c) Currently, no more than 12 EC prototypes have been developed so far in the world [33]. As maximal subclassification, they can be divided as based on the Solid-to-Solid Heat Transfer (SSHT) mechanism employing thermal diodes or the AeR cycles. Most of the prototypes are based on a linear mechanism for applying/removing stress, by means of a linear driver with a traction or compression operation. The pioneers of EC device developing were Cui et al. [33] in 2012 introducing the very first EC proof-of-concept for cooling, mounting NiTi wires (0.5 mm diameter) placed between two rings (the upper one is inclined). The rotation of the rings and the convective heat exchange with air ensures the exploitation of the AeR cooling cycle. The device achieved 17 K as maximum adiabatic temperature change (under 8.5% strain applied for stretching). The main problem of this device was the low lifetime of the refrigerant mounted with a high percentage of cracking. Subsequently, three more devices were presented to scientific community; all based on linear mechanism and mounting Ni-Ti alloys in different shapes [33]. Subsequently, in the late 2018, the German group of Saarland University, introduced [33] a new rotary EC prototype mounting wires of $Ni_{45}Ti_{47.25}Cu_5V_{2.75}$ whose fatigue life is long-er than the binary NiTi alloys and exhibiting a ΔT_{ad} of 28 K if loaded with a strain rate of 0.05 s^{-1} up to a maximum strain of 8.5%. Preliminary results on the device guaranteed 8.4 as COP and 250 W as cooling power with a total mass of 50 g of eCM.

Next to the applications devoted toward air conditioning and refrigeration, some pioneering groups explored the possibility of employing EC devices for applications at the miniature scale. Typical examples of miniature scale are microelectronic de-vices, smart sensors, and lab-on-a-chip systems, where the integration of various functionalities in small spaces leads to highly localized generation of heat requiring active temperature control.

A prototype oriented toward these goals was proposed by Bruederlin et al. [37] and based on a bridge system. In the device the eCM is moved up and down on a concave surface, with the double role of: i) showing eCE through bending/unbending since the tension applied to the wire/film makes it deflecting in the centre of its surface; ii) acting as a heat sink by conduction. It requires a single actuator to carry out the loading and unloading phases. The [37] system is SSHT type, and it has the disadvantage of mounting a small mass of eCM and so, to achieve small values of cooling power. In an updated version, Bruederlin et al. [37] developed a TiNiFe foil-based microscale device meeting the triple requirement of materials design, engineering and microtechnology.

In 2019, Greco et al. [33] realized a microscale device SSHT based where Ni-Ti wires are cyclically stretched and relaxed. The device is targeted in the range of small powers and 28.3 K is the highest temperature span achieved. Greco et al. developed [33] some miniature scale cooling demonstrators using SSHT showing a specific cooling power of 2.9 W g^{-1} and a COP of 3.2. Furthermore, next to the wires, the use of SMA films or foils is also a right solution as the large surface-to-volume ratios enable high cycling frequencies.

Even if the above-mentioned devices are all targeted on miniature scale, they are just proof-of-concepts and all of them are based on SSHT mechanism [38]. The gap in the EC research field that this project wants to fill is the development of a small-scale device not based on SSHT anymore, but realized through the concept of AeR (where air is the heat transfer fluid) and, at the same time specifically targeted on the cooling of electronic devices in terms of power demand, temperature range and size.

4. THE CHECK TEMPERATURE PROTOTYPE

The specific application toward CHECK TEMPERATURE is devoted to, is the cooling of data centres and power electronic components where, rather than the traditional finned systems, a more sophisticated cooling system is required.

As visible in Figure 3, the design of the prototype is characterized by small size and low weight (500 g weight, elastocaloric material included). The substantial difference lies in the method of load application: tensile and bending. The prototype based on bending [38] consists of two mini channels (an upper and a downer one) where wires of elastocaloric materials are located along the direction of the HTF since they are anchored to the ends through bars. A long bar system separates the two channels. As Figure 4 reports more in detail, a bending plate is in the centre of the channels, and it is responsible of the loading/unloading of the wires thanks to bending operation generated by up and down movements. HTF (air) flows in the channels and it releases heat when the caloric material is in the martensitic phase, whereas it absorbs heat when the caloric material is in the austenitic phase. Simultaneously, in the downer channel the inside wires should be arranged in an unloaded position (austenite) and the air would flow the opposite direction, thus transferring heat to the SMA wires. Dually, when the plate moves downwards there is the reverse behavior in the device: the wires located in the upper channel are unloaded whereas the ones of the downer are loaded. In this way, the useful effect of the refrigeration cycle will be obtained in half of the time of an entire AeR cycle. The device will be made of 240 wires of $Ni_{50.8}Ti_{49.2}$ alloy, for a total mass of 61g. The choice of $Ni_{50.8}Ti_{49.2}$ [39] must be attributed to the desire of make the device operating at room temperature range. In Table 1 the main EC characteristics of $Ni_{50.8}Ti_{49.2}$ are listed. Finally, in Figure 4 is reported a conceptual scheme of the proposed concept and the application.

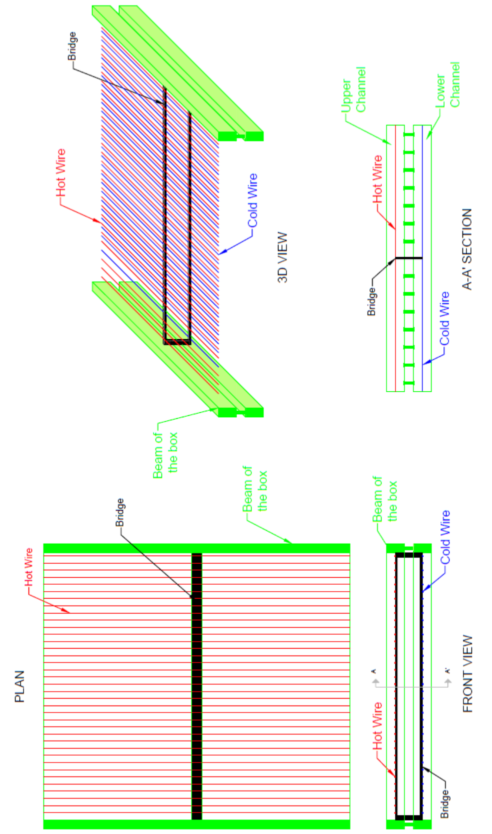

Figure 3. A schematic of the design of the CHECK TEMPERATURE device

Table 1. Elastocaloric characteristics of $Ni_{50.8}Ti_{49.2}$ [39]

Temperature [°C]	ΔT_{ad} [°C] (550 Mpa T_{ref} = 25°C)	Latent Heat [J/g]
A_f = -14.5	22.7 loading	16.9
A_s = -25.5	14 unloading	14.6
M_s = -38.1		
M_f = -51.2		

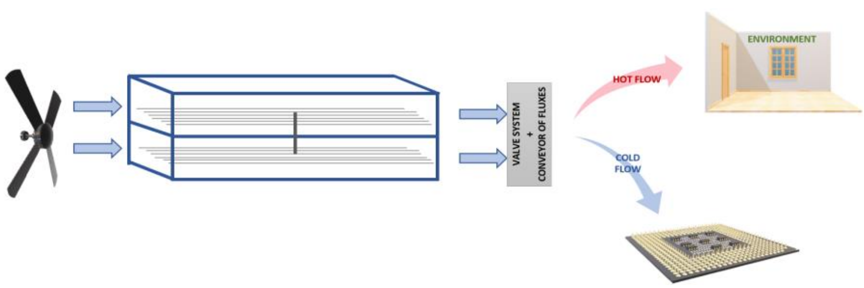

Figure 4. A panel of the proposed concept and the application

5. CONCLUSIONS

In this paper the CHECK TEMPERATURE project, financed by Department of Industrial Engineering of University of Naples Federico II, has been introduced. The device is characterized by a bridge design to locate 240 wires of $Ni_{50.8}Ti_{49.2}$ and to achieve a maximum cooling power of 50 W. The further steps of the project see the development of a numerical model to identify the most suitable design parameters and the best working conditions to drive the experimental realization. Then an experimental test campaign will take place and a map of performance would draw also with the help of the numerical model. In the end, the final goal will be the coupling of the device to a suitable electronic circuit to be cooled.

ACKNOWLEDGMENT

The paper is realized from the project CHECK TEMPEATURE that is financially supported by the 2021 internal grant reserved for Fixed-Term Research of Department of Industrial Engineering, University of Naples Federico II.

REFERENCES

[1] Qian, S., Nasuta, D., Rhoads, A., Wang, Y., Geng, Y., Hwang, Y., Radermacher, R., Takeuchi, I. (2016). Not-in-kind cooling technologies: A quantitative comparison of refrigerants and system performance. International Journal of Refrigeration, 62: 177-192. https://doi.org/10.1016/j.ijrefrig.2015.10.019

[2] Montreal Protocol on Substances That Deplete the Ozone Layer Final Act 1987. (1988). 22 INT'L L. 1263. https://scholar.smu.edu/til/vol22/iss4/21.

[3] Kyoto Protocol United Nations Framework Convention on Climate Change. (1977). Kyoto Prot. 19(8).

[4] Greco, A., Mastrullo, R., Palombo, A. (1997). R407C as an alternative to R22 in vapour compression plant: An experimental study. International Journal of Energy Research, 21(12): 1087-1098. https://doi.org/10.1002/(SICI)1099-114X(19971010)21:12<1087::AID-ER330>3.0.CO;2-Y

[5] Greco, A., Vanoli, G.P. (2006). Experimental two-phase pressure gradients during evaporation of pure and mixed refrigerants in a smooth horizontal tube. Comparison with correlations. Heat and Mass Transfer, 42(8): 709-725. https://doi.org/10.1007/s00231-005-0020-7

[6] Greco, A., Vanoli, G.P. (2004). Evaporation of refrigerants in a smooth horizontal tube: Prediction of R22 and R507 heat transfer coefficients and pressure drop. Applied Thermal Engineering, 24(14-15): 2189-2206. https://doi.org/10.1016/j.applthermaleng.2004.02.006

[7] Aprea, C., Greco, A. (2003). Performance evaluation of R22 and R407C in a vapour compression plant with reciprocating compressor. Applied Thermal Engineering, 23(2): 215-227. https://doi.org/10.1016/S1359-4311(02)00160-6

[8] Aprea, C., Greco, A., Rosato, A. (2008). Comparison of R407C and R417A heat transfer coefficients and pressure drops during flow boiling in a horizontal smooth tube. Energy Conversion and Management, 49(6): 1629-1636. https://doi.org/10.1016/j.enconman.2007.11.003

[9] Aprea, C., Greco, A., Maiorino, A. (2018). HFOs and their binary mixtures with HFC134a working as drop-in refrigerant in a household refrigerator: Energy analysis and environmental impact assessment. Applied Thermal Engineering, 141: 226-233. https://doi.org/10.1016/j.applthermaleng.2018.02.072

[10] Greco, A., Gundabattini, E., Gnanaraj, D.S., Masselli, C. (2020). A comparative study on the performances of flat plate and evacuated tube collectors deployable in domestic solar water heating systems in different climate areas. Climate, 8(6): 78. https://doi.org/10.3390/cli8060078

[11] Cascetta, F., Di Lorenzo, R., Nardini, S., Cirillo, L. (2017). A Trnsys simulation of a solar-driven air refrigerating system for a low-temperature room of an agro-industry site in the southern part of Italy. Energy Procedia, 126: 329-336. https://doi.org/10.1016/j.egypro.2017.08.259

[12] Barbato, M., Cirillo, L., Menditto, L., Moretti, R., Nardini, S. (2017). Geothermal energy application in Campi Flegrei Area: The case study of a swimming pool building. International Journal of Heat and Technology, 35: S102-S107. https://doi.org/10.18280/ijht.35Sp0114

[13] D'Agostino, D., Greco, A., Masselli, C., Minichiello, F. (2020). The employment of an earth-to-air heat exchanger as pre-treating unit of an air conditioning system for energy saving: A comparison among different worldwide climatic zones. Energy and Buildings, 229: 110517. https://doi.org/10.1016/j.enbuild.2020.110517

[14] Aprea, C., de Rossi, F., Greco, A., Renno, C. (2003). Refrigeration plant exergetic analysis varying the compressor capacity. International Journal of Energy Research, 27(7): 653-669. https://doi.org/10.1002/er.903

[15] Kitanovski, A., Plaznik, U., Tomc, U., Poredoš, A. (2015). Present and future caloric refrigeration and heat-pump technologies. International Journal of Refrigeration, 57: 288-298. https://doi.org/10.1016/j.ijrefrig.2015.06.008

[16] Aprea, C., Greco, A., Maiorino, A., Masselli, C. (2018). The environmental impact of solid-state materials working in an active caloric refrigerator compared to a vapor compression cooler. Int. J. Heat Technol, 36(4): 1155-1162. https://doi.org/10.18280/ijht.360401

[17] Aprea, C., Greco, A., Maiorino, A., Masselli, C. (2020). The use of barocaloric effect for energy saving in a domestic refrigerator with ethylene-glycol based nanofluids: A numerical analysis and a comparison with a vapor compression cooler. Energy, 190: 116404. https://doi.org/10.1016/j.energy.2019.116404

[18] Brück, E., Tegus, O., Thanh, D.C., Buschow, K.H.J. (2007). Magnetocaloric refrigeration near room temperature. Journal of Magnetism and Magnetic Materials, 310(2): 2793-2799. https://doi.org/10.1016/j.jmmm.2006.10.1146

[19] Aprea, C., Greco, A., Maiorino, A., Masselli, C. (2017). Analyzing the energetic performances of AMR regenerator working with different magnetocaloric materials: Investigations and viewpoints. Int. J. Heat Technol, 35(Sp.1): S383-S390. https://doi.org/10.18280/ijht.35Sp0152

[20] Aprea, C., Greco, A., Maiorino, A. (2011). A numerical analysis of an active magnetic regenerative cascade

system. International Journal of Energy Research, 35(3): 177-188. https://doi.org/10.1002/er.1682

[21] Aprea, C., Greco, A., Maiorino, A., Masselli, C. (2016). A comparison between different materials in an active electrocaloric regenerative cycle with a 2D numerical model. International Journal of Refrigeration, 69: 369-382. https://doi.org/10.1016/j.ijrefrig.2016.06.016

[22] Shi, J., Han, D., Li, Z., et al. (2019). Electrocaloric cooling materials and devices for zero-global-warming-potential, high-efficiency refrigeration. Joule, 3(5): 1200-1225. https://doi.org/10.1016/j.joule.2019.03.021

[23] Chen, J., Lei, L., Fang, G. (2021). Elastocaloric cooling of shape memory alloys: A review. Materials Today Communications, 28: 102706. https://doi.org/10.1016/j.mtcomm.2021.102706

[24] Aprea, C., Greco, A., Maiorino, A., Masselli, C. (2019). Enhancing the heat transfer in an active barocaloric cooling system using ethylene-glycol based nanofluids as secondary medium. Energies, 12(15): 2902. https://doi.org/10.3390/en12152902

[25] Kabirifar, P., Žerovnik, A., Ahčin, Ž., Porenta, L., Brojan, M., & Tušek, J. (2019). Elastocaloric cooling: state-of-the-art and future challenges in designing regenerative elastocaloric devices. Strojniski Vestnik/Journal of Mechanical Engineering, 65(11-12): 615-630. https://doi.org/10.5545/sv-jme.2019.6369

[26] Cirillo, L., Greco, A., Masselli, C. (2022). Cooling through barocaloric effect: A review of the state of the art up to 2022. Thermal Science and Engineering Progress, 33: 101380. https://doi.org/10.1016/j.tsep.2022.101380

[27] Moya, X., Kar-Narayan, S., Mathur, N.D. (2014). Caloric materials near ferroic phase transitions. Nature materials, 13(5): 439-450. https://doi.org/10.1038/nmat3951

[28] Müller, I., Seelecke, S. (2001). Thermodynamic aspects of shape memory alloys. Mathematical and Computer Modelling, 34(12-13): 1307-1355. https://doi.org/10.1016/S0895-7177(01)00134-0

[29] Frenzel, J., Wieczorek, A., Opahle, I., Maaß, B., Drautz, R., & Eggeler, G. (2015). On the effect of alloy composition on martensite start temperatures and latent heats in Ni–Ti-based shape memory alloys. Acta Materialia, 90: 213-231. https://doi.org/10.1016/j.actamat.2015.02.029

[30] Pecharsky, V.K., Gschneidner Jr, K.A. (1999). Magnetocaloric effect and magnetic refrigeration. Journal of Magnetism and Magnetic Materials, 200(1-3): 44-56. https://doi.org/10.1016/S0304-8853(99)00397-2

[31] Aprea, C., Greco, A., Maiorino, A., Masselli, C. (2017). A comparison between electrocaloric and magnetocaloric materials for solid state refrigeration. International Journal of Heat and Technology, 35(1): 225-234. https://doi.org/10.18280/ijht.350130

[32] Aprea, C., Greco, A., Maiorino, A., Masselli, C. (2018). Energy performances and numerical investigation of solid-state magnetocaloric materials used as refrigerant in an active magnetic regenerator. Thermal Science and Engineering Progress, 6: 370-379. https://doi.org/10.1016/j.tsep.2018.01.006

[33] Greco, A., Aprea, C., Maiorino, A., Masselli, C. (2019). A review of the state of the art of solid-state caloric cooling processes at room-temperature before 2019. International Journal of Refrigeration, 106: 66-88. https://doi.org/10.1016/j.ijrefrig.2019.06.034

[34] Qian, S., Geng, Y., Wang, Y., Ling, J., Hwang, Y., Radermacher, R., Takeuchi, I., Cui, J. (2016). A review of elastocaloric cooling: Materials, cycles and system integrations. International Journal of Refrigeration, 64: 1-19. https://doi.org/10.1016/j.ijrefrig.2015.12.001

[35] Cirillo, L., Farina, A.R., Greco, A., Masselli, C. (2021). Numerical optimization of a single bunch of NiTi wires to be placed in an elastocaloric experimental device: Preliminary Results. Magnetochemistry, 7(5): 67. https://doi.org/10.3390/magnetochemistry7050067

[36] Cirillo, L., Farina, A.R., Greco, A., Masselli, C. (2022). The optimization of the energy performances of a single bunch of elastocaloric elements to be employed in an experimental device. Thermal Science and Engineering Progress, 27: 101152. https://doi.org/10.1016/j.tsep.2021.101152

[37] Bruederlin, F., Ossmer, H., Wendler, F., Miyazaki, S., Kohl, M. (2017). SMA foil-based elastocaloric cooling: from material behavior to device engineering. Journal of Physics D: Applied Physics, 50(42): 424003. https://doi.org/10.1088/1361-6463/aa87a2

[38] Sharar, D.J., Radice, J., Warzoha, R., Hanrahan, B., Smith, A. (2021). Low-force elastocaloric refrigeration via bending. Applied Physics Letters, 118(18): 184103. https://doi.org/10.1063/5.0041500

[39] Zhou, M., Li, Y., Zhang, C., Li, S., Wu, E., Li, W., Li, L. (2018). The elastocaloric effect of Ni50. 8Ti49. 2 shape memory alloys. Journal of Physics D: Applied Physics, 51(13): 135303. https://doi.org/10.1088/1361-6463/aaafc2

NOMENCLATURE

A	Temperature of austenite phase, K
C	specific heat, J. kg^{-1}. K^{-1}
M	Tempearture of martensite phase, K
T	Temperature, K

Greek symbols

Δ	finite difference
ε	strain, %
σ	stress, MPa

Subscripts

0	initial
1	final
ad	adiabatic
f	finish
ref	reference
s	start